Ultrafast optical spectroscopy of the lowest energy excitations in the Mott insulator compound YVO3

Novelli, Fabio; Fausti, Daniele; Reul, Julia; Cilento, Federico; van Loosdrecht, Paul H. M.; Nugroho, Agung A.; Palstra, Thomas; Grueninger, Markus; Parmigiani, Fulvio

Published in:
Physical Review. B: Condensed Matter and Materials Physics

DOI:
10.1103/PhysRevB.86.165135

Hubbard exciton revealed by time-domain optical spectroscopy in YVO_3: supplementary material

Fabio Novelli,[1] Daniele Fausti,[1,2,*] Julia Reul,[3] Federico Cilento,[2] Paul H. M. van Loosdrecht,[4] Agung A. Nugroho,[5] Thomas T. M. Palstra,[4] Markus Grüninger,[3] and Fulvio Parmigiani[1,2]

[1]*Department of Physics, Università degli Studi di Trieste, 34127 Trieste, Italy*
[2]*Sincrotrone Trieste S.C.p.A., 34127 Basovizza, Italy*
[3]*Department of Physics, University of Cologne, 50923 Köln, Germany*
[4]*Zernike Institute for Advanced Materials, University of Groningen, 9747 AG Groningen, The Netherlands*
[5]*Faculty of Mathematics and Natural Sciences, Jl. Ganesa 10 Bandung, 40132, Indonesia*

(Dated: October 11, 2012)

I. TIME-RESOLVED MEASUREMENTS

We measured the transient reflectivity $\Delta R(t)/R$ as a function of temperature and pump-probe delay in the 450-750 nm wavelength-region after excitation with 4 mJ/cm^2 of 775 nm ultra-short Ti:Sa laser pulses at 40 KHz. The linearity of the response was checked in all phases. Time-domain measurements were performed with the pump parallel to the a-axis (P||a) and probe parallel to c (p||c) for the intervals -2÷4 ps and 4÷1000 ps. A set of representative measurements is plotted on FIG. 1. Similar measurements performed with pump parallel to the c-axis (P||c) and probe parallel to the a-axis (p||a) show only a temperature-independent fast decay time (FIG. 2). Long timescale measurements for P||a and p||c are shown in FIG. 3.

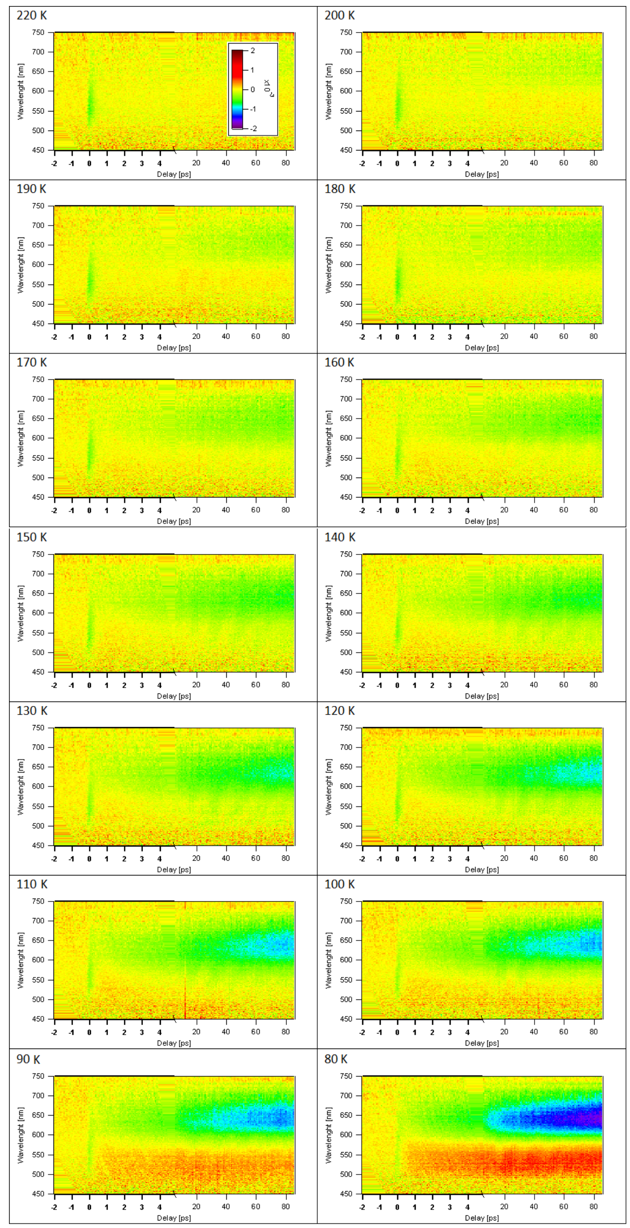

FIG. 1: Relative variation of the reflectivity in the -2 to 80 ps range, with P||a and p||c.

II. TIME-RESOLVED FITTING

We fitted the transient reflectivity in the time- and frequency- domains by allowing the variation of only 4 parameters out of 21: the optical strength of SP, and the optical strength, width, and central frequency of HE. The most relevant parameters are the oscillator strength of the SP peak, the oscillator strength and the width of the HE peak. Above $200\,K$ all the transients observed can be described by changing only the strength of the SP peak, while the strength of the HE becomes more and more relevant upon cooling below $200\,K$. At $80\,K$, the strength of the SP drops of about 1% on the fast timescale ($< 1\,ps$) and increases of about 1% for longer times ($40-80\,ps$). The other parameters are necessary to account for the long dynamics below $200\,K$. The strength and width of HE show a drop lower than 0.5% in the region investigated, while the cental frequency is virtually unchanged at all temperatures ($< 0.02\%$). From the full set of time-dependent parameters obtanied we calculated the spectral weight of each band separately by numerical integration in the $0-2.85\,eV$ ($0-23000\,cm^{-1}$) range, as described in the paper.

It should be noted that the central frequency of the HE for the static data shifts of a few % by changing temperature. This confirms that even though structural

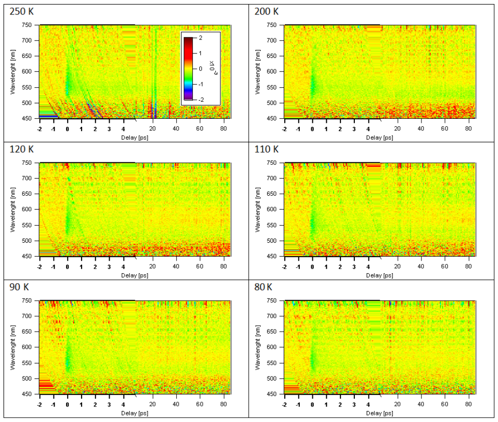

FIG. 2: Measurements with P||c and p||a.

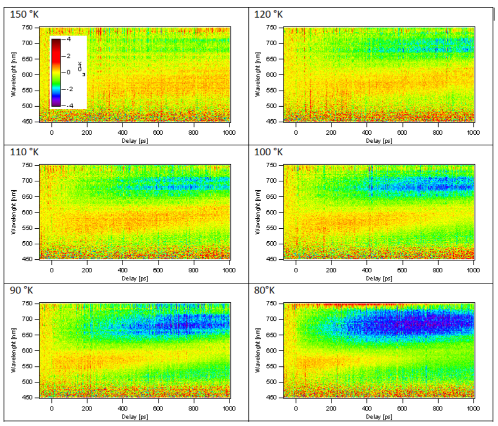

FIG. 3: Relative variation of the reflectivity in the -40 to 1000 ps range, with P||a and p||c.

distortions may be of relevance in determining the ratio between the SW of HE and SP at equilibrium they are not the main player in the dynamical response.

III. NON-THERMAL CONTRIBUTION

At any fixed temperature T, the non-thermal contribution to the variations of the SW of HE and SP can be calculated from static optical properties, the time-resolved data and the laser pump energy, as follows:

$\Delta SW^{non-thermal}(t) = SW^{pumped}(t) - SW^{static}(T + \Delta T(t))$,

where $SW^{pumped}(t)$ is the photo-excited SW and $SW^{static}(T + \Delta T(t))$ is obtained by interpolation at $T + \Delta T(t)$ of the static model. $\Delta T(t)$ is the pump-induced heating calculated from a two-temperature model (2TM)[2,3] for the lattice (L) and spin (S) degrees of freedom:

$C_L \frac{dT_L}{dt} = -\gamma(T_L - T_S) + \rho P_{eff}(t)$

$C_S \frac{dT_S}{dt} = -\gamma(T_S - T_L) + (1-\rho) P_{eff}(t)$

where C_L and C_S are the heat capacities[4] of the two subsystems, $\gamma = 10^{-5} W/(K \cdot mol)$ and $\rho = 0.93$ are phenomelogical constants describing, respectively, the magnetoelastic coupling[5] and the coupling of the electronic subsystem to the other two. In this model we assume that the pump pulse $P(t)$ photo-excites carriers from the lower Hubbard band (LHB) to the upper Hubbard band (UHB). As the quasi-particles relax, they act as an effective pump $P_{eff}(t)$ for the lattice and spin degrees. The behaviour of T_L and T_S is reported in FIG. 4 for T=80 K.

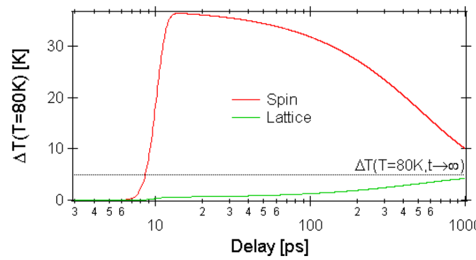

FIG. 4: Two temperature model for T=80 K. A gaussian $P_{eff}(t)$ with $FWHM = 3\,ps$ is turned on at $t = 10\,ps$. $T_S(t)$ is reported in red, $T_L(t)$ in green while the converging straight line $\Delta T(80\,K, t \to \infty)$ is dotted.

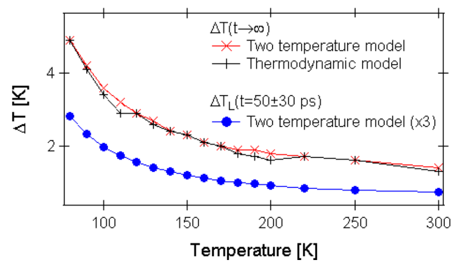

FIG. 5: Comparison of the two thermodynamic models at equilibrium or long pump-probe delay. The blue dots represent the calculated lattice temperature used to calculate the non-thermal contribution to the SW variations at different temperatures.

The validity of this model is confirmed by comparison, at any temperature, with the expected thermodynamic steady-state temperature increase $\widetilde{\Delta T(T)}$. It is straightforward to write

$\widetilde{\Delta T(T)} = \frac{Q_{abs} \cdot N_A \cdot V}{S \cdot d \cdot u \cdot C_{mol}} \approx \frac{150}{C_{mol}[J/(mol \cdot K)]}$,

where Q_{abs} is the pump energy absorbed by the sample, N_A the Avogadro's number, V the elementary cell volume, S the sample's surface irradiated, d the pump's penetration depth, u the number of chemical units in a cell and C_{mol}[4] the temperature-dependent total heat capacity. There is a good agreement between the temperature dependence of the temperature increases for the two models, as shown in FIG. 5 (red and black curves). At this point, the 2TM permits to obtain the temporal dependence of the lattice temperature and allows for the calculation of the non-thermal component. The blue dots in FIG. 5 represent the temperature variations at pump-probe delay $t = 50\,ps$ used to obtain the non-thermal contribution to the variation of the spectral weight (FIG.6 in the paper).

* Electronic address: `daniele.fausti@elettra.trieste.it`

[1] J. Reul et al. preprint arXiv:1205.5048, accepted Phys. Rev. B , (2012).

[2] A. Kirilyuk, A. Kimel, and T. Rasing Rev. Mod. Phys. **82**, 2742 (2010).

[3] E. Beaurepaire, J.-C. Merle, A. Daunois, and J.-Y. Bigot Phys. Rev. Lett. **76**, 4250 (1996).

[4] G.R. Blake, T.T.M. Palstra, Y. Ren, A.A. Nugroho, A.A. Menovsky Phys. Rev. B **65**, 174112 (2002).

[5] C. Marquina, M. Sikora, M.R. Ibarra, A.A. Nugroho, T.T.M. Palstra Journal of Magnetism and Magnetic Materials **290**, 428 (2005).